

Translational Diffusion of Polymer Chains with Excluded Volume and Hydrodynamic Interactions by Brownian Dynamics Simulation

Bo Liu and Burkhard Dünweg*

*Max-Planck-Institut für Polymerforschung
Ackermannweg 10, D-55128 Mainz, Germany*

(November 7, 2018)

Within Kirkwood theory, we study the translational diffusion coefficient of a single polymer chain in dilute solution, and focus on the small difference between the short-time Kirkwood value $D^{(K)}$ and the asymptotic long-time value D . We calculate this correction term by highly accurate large-scale Brownian Dynamics simulations, and show that it is in perfect agreement with the rigorous variational result $D < D^{(K)}$, and with Fixman’s Green-Kubo formula, which is re-derived. This resolves the puzzle posed by earlier numerical results (Rey *et al.*, *Macromolecules* 24, 4666 (1991)), which rather seemed to indicate $D > D^{(K)}$; the older data are shown to have insufficient statistical accuracy to resolve this question. We then discuss the Green-Kubo integrand in some detail. This function behaves very differently for pre-averaged vs. fluctuating hydrodynamics, as shown for the initial value by analytical considerations corroborated by numerical results. We also present further numerical data on the chain’s statics and dynamics.

I. INTRODUCTION

Diffusion of polymer chains in dilute solution has been a subject of substantial theoretical interest^{1–11}. A particularly important result is the Kirkwood formula for the translational diffusion coefficient of a molecule immersed in a solvent of temperature T and viscosity η ,

$$D^{(K)} = \frac{D_0}{N} + \frac{k_B T}{6\pi\eta} \left\langle \frac{1}{R_H} \right\rangle. \quad (1)$$

Here k_B denotes Boltzmann’s constant, while N is the number of chain segments, each of which has a segmental diffusion coefficient $D_0 = k_B T / \zeta$, where ζ is the segmental friction coefficient, $\zeta = 6\pi\eta a$, where a denotes the segment’s Stokes radius. R_H is the hydrodynamic radius of the molecule, which is defined as a thermal average over the inverse intramolecular distances between segments:

$$\left\langle \frac{1}{R_H} \right\rangle = \frac{1}{N^2} \sum_{i \neq j} \left\langle \frac{1}{r_{ij}} \right\rangle. \quad (2)$$

Equation 1 is not exact, but rather the result of a number of approximations¹¹. Firstly, the Brownian motion of the molecule is described by a Smoluchowski equation (Kirkwood’s diffusion equation) in the space of the segment coordinates \vec{r}_i . Secondly, the diffusion tensor $\overleftrightarrow{D}_{ij}$, whose off-diagonal elements describe the hydrodynamic interaction between segments i and j , is approximated by the Oseen formula,

$$\overleftrightarrow{D}_{ij} = \frac{k_B T}{\zeta} \delta_{ij} \overleftrightarrow{1} + (1 - \delta_{ij}) \frac{k_B T}{8\pi\eta r_{ij}} \left(\overleftrightarrow{1} + \hat{r}_{ij} \otimes \hat{r}_{ij} \right), \quad (3)$$

where \hat{r}_{ij} is the unit vector in direction of $\vec{r}_{ij} = \vec{r}_i - \vec{r}_j$. Thirdly, the diffusion coefficient is evaluated in the *short-time limit* of the Smoluchowski equation. The diffusion coefficient in the asymptotic long-time limit, which we denote as D , is *different* from the short-time value $D^{(K)}$, due to the presence of intramolecular dynamic correlations, which are expected to decay on the time scale of the overall relaxation time of the chain’s conformational degrees of freedom (the Zimm time τ_Z). Thus, the behavior on short time scales $t \ll \tau_Z$ is governed by $D^{(K)}$, while on long time scales $t \gg \tau_Z$ the diffusive motion takes place with the coefficient D . For a general diffusion tensor (not necessarily of the Oseen type) the same considerations apply. In this case the short-time diffusion coefficient is obtained by averaging over the trace:

$$D^{(K)} = \frac{1}{3N^2} \sum_{ij} \text{Tr} \left\langle \overleftrightarrow{D}_{ij} \right\rangle; \quad (4)$$

in what follows, the term “Kirkwood formula” will always refer to Eq. 4.

The difference between $D^{(K)}$ and D has caused considerable interest and some confusion (see below); it is the purpose of the present paper to contribute to the clarification of these questions. Both light scattering experiments^{12–15} and first-principles Molecular Dynamics (MD) simulations^{16,17} show that the difference must be quite small such that it is below resolution. In the case of MD, the main difficulty is the fact that the “short-time” limit of Kirkwood theory is of course not the exact $t \rightarrow 0$ limit, but rather a time regime where the

*Electronic mail: duenweg@mpip-mainz.mpg.de

local motions of the particles in their “cages” (or the momenta) have already relaxed completely, while the conformational degrees of freedom of the chain must at the same time be considered as completely unrelaxed. To reach this separation of time scales (i. e. ballistic / short-time diffusive / long-time diffusive) in an unambiguous fashion would require extremely long chains which are not accessible to today’s computer power. A related problem is the fact that the monomer diffusion coefficient D_0 , which must be taken into account in order to evaluate $D^{(K)}$ correctly¹⁷, is a somewhat fuzzy and ill-defined object in MD. This is seen in a quite obvious fashion when looking at the velocity autocorrelation function of a single monomer, whose time integral is the chain diffusion constant D ¹⁸: After a rather quick short-time decay, one gets a negative tail which slowly decays to zero on the time scale of the overall relaxation of the chain as a whole¹⁹. This latter decay describes the Rouse- or Zimm-like slowing down by the coupling to the other monomers, while the quick short-time regime defines, in principle, the monomer diffusion coefficient D_0 . However, there is no obvious and well-defined time which discriminates between short- and long-time regime. Depending on where this “cut” is being put, one obtains slightly different values for D_0 . This latter problem does not exist in a recently introduced hybrid approach²⁰, where the chain monomers are coupled dissipatively to a discretized hydrodynamic background, such that the monomer diffusion coefficient is an input parameter. However, the former problem (lack of separation of time scales) is still present.

In order to cope with these difficulties, one therefore has to work *strictly within* the framework of Kirkwood theory (i. e. the Smoluchowski equation), such that D_0 is just an input parameter, the ballistic regime does not exist, and the theory has a well-defined diffusive short-time limit. Nevertheless, calculating the long-time diffusion coefficient D , and the smooth crossover between the short-time behavior governed by $D^{(K)}$, and the long-time regime governed by D , requires to actually solve the Smoluchowski equation. However, closed analytical solutions do not exist as soon as fluctuating hydrodynamic interactions and / or excluded volume interactions are introduced. For this reason, analytical progress on the problem has been limited; nevertheless, a few important results have been obtained. Within the preaveraged approximation, Öttinger²¹ derived a closed expression for D which clearly differs from $D^{(K)}$. Furthermore, it is possible to establish rigorous variational bounds on transport coefficients^{11,22,23}, from which one can show that D must be *smaller* than $D^{(K)}$. Moreover, Fixman²⁴ derived the Green-Kubo type relation

$$D = D^{(K)} - D_1 \quad (5)$$

with

$$D_1 = \frac{1}{3N^2} \int_0^\infty dt \langle \vec{A}(0) \cdot \vec{A}(t) \rangle > 0 \quad (6)$$

and

$$\vec{A} = \sum_{ij} \overleftrightarrow{\mu}_{ij} \cdot \vec{F}_j, \quad (7)$$

where \vec{F}_j is the force acting on segment j , and $\overleftrightarrow{\mu}_{ij}$ is the mobility tensor, $\overleftrightarrow{\mu}_{ij} = \overleftrightarrow{D}_{ij}/(k_B T)$.

However, for a more quantitative understanding one has to rely on numerical solutions of the Smoluchowski equation. The most common approach is Brownian Dynamics (BD) simulations, which, for the case of fluctuating hydrodynamic interactions, was pioneered by Ermak and McCammon²⁵. BD simulations for polymer chains have been done by numerous workers before^{24,26–36}. One of these studies³¹ produced quite accurate data, which however seemed to indicate $D > D^{(K)}$. No satisfactory explanation of this deviation has been given so far. For this reason, we have looked into the problem again, and performed careful BD simulations of the same model with identical parameters. In this model, excluded volume interactions are represented by a relatively soft potential, while the hydrodynamic interactions are modeled via the Rotne-Prager-Yamakawa (RPY) tensor^{22,37}.

As noted before³¹, this is a numerically demanding task, as such a calculation is looking for a rather small effect. One has, on the one hand, to watch out for discretization errors due to the finite time step³¹, and, on the other hand, to make sure that the statistical accuracy of the data suffices. In order to test the relation $D = D^{(K)} - D_1$, all three quantities must be determined independently. As our analysis shows (see below), it turns out that both $D^{(K)}$ and D_1 can be calculated with moderate statistical effort, and Ref. 31 has indeed obtained values which coincide with ours. The diffusion coefficient D itself, however, is subject to much larger fluctuations, such that its accurate determination needs substantially more computer power than what was available to the authors of Ref. 31. We believe that this is the most likely explanation of the deviation, which is not confirmed by our much more accurate data (these are based on an observation time which is orders of magnitude larger than that of Ref. 31). Rather, we find a very nice agreement with the relation $D = D^{(K)} - D_1$ with $D_1 > 0$. We also re-derive Fixman’s²⁴ Green-Kubo formula for D_1 , Eq. 6, by means of an alternative approach based on the Mori-Zwanzig projection operator technique, and try to elucidate its relation to the stochastic analog of the velocity autocorrelation function. Furthermore, we attempt to discuss the scaling behavior of D_1 via both scaling arguments and numerical data; here we have obtained some results which we view as somewhat unexpected and counter-intuitive. However, these should be considered as preliminary and inconclusive. The computational demands of the calculations are so large that it is impossible to accurately study the dynamics for chain lengths much beyond $N \sim 10^2$, which is

clearly not long enough to justify any claim of asymptotic behavior.

The outline of this article is as follows. In Sec. II we define the simulated model and describe the simulation procedure we applied. In Sec. III we derive the short-time diffusion coefficient and long-time diffusion coefficient from the mean square displacement of the center of mass, and compare the analytical predictions with the numerical results. Section IV presents our considerations concerning the scaling of the correction term D_1 together with numerical data. Section V then discusses further data on the static and dynamic scaling properties, mainly to demonstrate the consistency of the results. In Sec. VI we conclude with some final remarks.

II. MODEL AND SIMULATION METHOD

A. Bead-Spring Model

Following Rey *et al.*³¹, we have modeled the flexible polymer as a linear chain constituted by N units ranging from $N = 6$ to 200, each one connected with its first neighbors by means of harmonic springs. Therefore the bond lengths follow a Gaussian distribution whose variance we denote by b^2 , i. e. b is the statistical segment length. Excluded volume forces only act between non-neighboring units; they are introduced by means of a potential of the form $A \exp(-\beta r_{ij})$, where A and β are constant parameters. This potential is cut off at a distance r_c .

B. Hydrodynamic Interaction

The hydrodynamic interaction is introduced through the diffusion tensor proposed by Rotne and Prager and Yamakawa (RPY)^{22,37},

$$\overset{\leftrightarrow}{D}_{ij} = \begin{cases} \frac{k_B T}{6\pi\eta a} \overset{\leftrightarrow}{\mathbb{1}} & i = j \\ \frac{k_B T}{8\pi\eta r_{ij}} \left[\left(\overset{\leftrightarrow}{\mathbb{1}} + \hat{r}_{ij} \otimes \hat{r}_{ij} \right) + \frac{2a^2}{r_{ij}^2} \left(\frac{1}{3} \overset{\leftrightarrow}{\mathbb{1}} - \hat{r}_{ij} \otimes \hat{r}_{ij} \right) \right], & i \neq j \text{ and } r_{ij} \geq 2a \\ \frac{k_B T}{6\pi\eta a} \left[\left(1 - \frac{9}{32} \frac{r_{ij}}{a} \right) \overset{\leftrightarrow}{\mathbb{1}} + \frac{3}{32} \frac{r_{ij}}{a} \hat{r}_{ij} \otimes \hat{r}_{ij} \right], & i \neq j \text{ and } r_{ij} < 2a \end{cases} \quad (8)$$

where a is the Stokes radius of the beads. This tensor is positive-definite for all chain configurations.

C. Algorithm

The polymer motion is governed by the stochastic differential equation that we solve through the first-order Ermak and McCammon algorithm²⁵,

$$\vec{r}_i(t+h) = \vec{r}_i(t) + \sum_j \overset{\leftrightarrow}{\mu}_{ij} \cdot \vec{F}_j h + \vec{\rho}_i, \quad (9)$$

where h is the time step, \vec{F}_i the force on monomer i , $\overset{\leftrightarrow}{\mu}_{ij} = \overset{\leftrightarrow}{D}_{ij}/(k_B T)$, and $\vec{\rho}_i$ a random displacement with zero mean and variance-covariance matrix given by

$$\langle \vec{\rho}_i \otimes \vec{\rho}_j \rangle = 2 \overset{\leftrightarrow}{D}_{ij} h. \quad (10)$$

We generated the random terms $\vec{\rho}_i$ from a uniform distribution³⁸, and used the procedure given in Ref. 25 to satisfy Eq. 10. The term $h \sum_j (\partial/\partial \vec{r}_j) \cdot \overset{\leftrightarrow}{D}_{ij}$ on the right hand side of Eq. (9) was omitted, because the RPY tensor, due to the incompressibility of the solvent, is divergence-free, $(\partial/\partial \vec{r}_j) \cdot \overset{\leftrightarrow}{D}_{ij} = 0$.

D. Simulation Details

As in Ref. 31, we use a unit system where the three quantities b , $k_B T$, and $\zeta = 6\pi\eta a$ are set to unity. Hence the time unit is given by $\zeta b^2/k_B T$. In this unit system, the other parameters are $A = 75$, $\beta = 4$, $r_c = 0.512$, and $a = 0.256$. We used a reduced time step of $h = 0.005$, which is twice as small as that of Ref. 31. This choice was motivated by a comparison of end-to-end distance and gyration radius data obtained by simulations with various h with the corresponding data from Monte Carlo runs. This comparison showed that highly accurate results require a rather conservative h value.

For $N \leq 50$, data with good statistics were generated by the following procedure: (i) Equilibration by BD without hydrodynamic interactions, (ii) short additional equilibration with hydrodynamic interactions turned on, and (iii) a long BD production run. Furthermore, we averaged over five independent such runs. For these chains, the resulting total simulation time divided by the longest relaxation time τ_Z (which can be obtained from the time autocorrelation function of the end-to-end distance) is 0.5×10^6 for $N \leq 35$, 0.4×10^6 for $N = 40$, 0.3×10^6 for $N = 45$, and 0.2×10^6 for $N = 50$. All the statistical error bars were estimated by the blocking method developed by Flyvbjerg and Petersen³⁹.

From the results for these chains, it turned out that the dynamics on short time scales significantly below τ_Z is of particular interest (see below). For this reason, we studied two longer chains ($N = 100$ and 200) by a somewhat different procedure: By an efficient Monte Carlo procedure (the pivot algorithm^{40,41} combined with local moves) we generated a large sample of statistically independent conformations (128 conformations for $N = 100$, 3700 conformations for $N = 200$), from which we started BD runs with hydrodynamic interactions of short to moderate length (in our time units: $\tau = 2.5 \times 10^4$ for $N = 100$, $\tau = 100$ for $N = 200$). Although this implies a quite good statistical accuracy, it is nevertheless significantly worse than for the shorter chains. Therefore only the most

important and interesting properties were evaluated for $N = 100$ and 200 .

For chain length $N = 6$, our program needed 60 sec. to run 10^5 BD steps on a 667 MHz PC. This number of course strongly increases with N (~ 500 sec. for $N = 50$, $\sim 10^5$ sec. for $N = 200$); the asymptotic N^3 scaling of the algorithm was observed for (roughly) $N \geq 30$. The calculations ran for several months on a 16-machine PC cluster; the overall effort of the project in terms of single-processor time is estimated as roughly 6.7 years.

III. TRANSLATIONAL DIFFUSION COEFFICIENT

A. Theory

In order to calculate the translational diffusion coefficient in the short- and long-time regimes, we study the mean square displacement of the center of mass,

$$\vec{R}_{CM} = \frac{1}{N} \sum_i \vec{r}_i. \quad (11)$$

From the Ermak-McCammon algorithm, Eq. 9, we find the updating rule for \vec{R}_{CM} in one time step:

$$\begin{aligned} \Delta \vec{R}(t) &\equiv \vec{R}_{CM}(t+h) - \vec{R}_{CM}(t) \\ &= \frac{1}{N} \left(h\vec{A}(t) + h^{1/2}\vec{B}(t) \right), \end{aligned} \quad (12)$$

where we have introduced the abbreviations

$$\vec{A} = \sum_{ij} \overleftrightarrow{\mu}_{ij} \cdot \vec{F}_j \quad (13)$$

(this definition is identical to the notation of Fixman²⁴) and

$$\vec{B} = h^{-1/2} \sum_i \vec{\rho}_i. \quad (14)$$

Note that \vec{A} and \vec{B} are defined in such a way that they are independent of the time step h . As \vec{A} and \vec{B} , evaluated at the same time, are uncorrelated, and since $\langle \vec{B} \rangle$ vanishes, we find

$$\begin{aligned} \langle (\Delta \vec{R})^2 \rangle &= \frac{h}{N^2} \langle \vec{B}^2 \rangle + \frac{h^2}{N^2} \langle \vec{A}^2 \rangle \\ &= \frac{2h}{N^2} \sum_{ij} \text{Tr} \langle \overleftrightarrow{D}_{ij} \rangle + O(h^2). \end{aligned} \quad (15)$$

Thus the short-time diffusion coefficient is just given by the Kirkwood formula:

$$\begin{aligned} D^{short} &= \lim_{h \rightarrow 0} \frac{1}{6h} \langle (\Delta \vec{R})^2 \rangle \\ &= \frac{1}{3N^2} \sum_{ij} \text{Tr} \langle \overleftrightarrow{D}_{ij} \rangle \equiv D^{(K)}. \end{aligned} \quad (16)$$

For longer times (n time steps) we evaluate the mean square displacement as

$$\begin{aligned} &\left\langle \left(\vec{R}_{CM}(nh) - \vec{R}_{CM}(0) \right)^2 \right\rangle \\ &= \left\langle \left(\sum_{k=0}^{n-1} \Delta \vec{R}(kh) \right)^2 \right\rangle = \sum_{kl} \langle \Delta \vec{R}(kh) \cdot \Delta \vec{R}(lh) \rangle. \end{aligned} \quad (17)$$

The matrix with elements $\langle \Delta \vec{R}(kh) \cdot \Delta \vec{R}(lh) \rangle$ is obviously symmetric. Since all elements with constant $k-l$ are identical, for reasons of translational symmetry in time, we can simplify the previous expression as

$$\begin{aligned} &\left\langle \left(\vec{R}_{CM}(nh) - \vec{R}_{CM}(0) \right)^2 \right\rangle \\ &= n \langle \Delta \vec{R}(0)^2 \rangle + 2 \sum_{k=1}^{n-1} (n-k) \langle \Delta \vec{R}(0) \cdot \Delta \vec{R}(kh) \rangle. \end{aligned} \quad (18)$$

This is quite analogous to the standard relation between mean square displacement and velocity autocorrelation function¹⁸. In the long-time limit $n \rightarrow \infty$ we thus obtain a diffusion coefficient which still depends on the time step:

$$\begin{aligned} D^{long}(h) &= \lim_{n \rightarrow \infty} \frac{1}{6nh} \left\langle \left(\vec{R}_{CM}(nh) - \vec{R}_{CM}(0) \right)^2 \right\rangle \\ &= D^{(K)} + \frac{h}{6N^2} \langle \vec{A}^2 \rangle \\ &\quad + \frac{1}{3h} \sum_{k=1}^{\infty} \langle \Delta \vec{R}(0) \cdot \Delta \vec{R}(kh) \rangle; \end{aligned} \quad (19)$$

here we have assumed, as usual, that the correlation function decays quickly to zero.

We now make use of the fact that the stochastic terms \vec{B} are uncorrelated at different times, and that there is a correlation between \vec{A} and \vec{B} only if \vec{A} is evaluated at a *later* time as \vec{B} (of course, a stochastic “kick” at a certain time will influence how the system evolves dynamically in the future). We thus obtain for $k \geq 1$

$$\begin{aligned} \langle \Delta \vec{R}(0) \cdot \Delta \vec{R}(kh) \rangle &= \frac{h^2}{N^2} \langle \vec{A}(0) \cdot \vec{A}(kh) \rangle \\ &\quad + \frac{h^{3/2}}{N^2} \langle \vec{B}(0) \cdot \vec{A}(kh) \rangle, \end{aligned} \quad (20)$$

yielding the relation

$$D^{long}(h) = D^{(K)} + D_1(h) + D_2(h) \quad (21)$$

with

$$D_1(h) = \frac{h}{6N^2} \langle \vec{A}^2 \rangle + \frac{h}{3N^2} \sum_{k=1}^{\infty} \langle \vec{A}(0) \cdot \vec{A}(kh) \rangle \quad (22)$$

and

$$D_2(h) = \frac{h^{1/2}}{3N^2} \sum_{k=1}^{\infty} \left\langle \vec{B}(0) \cdot \vec{A}(kh) \right\rangle. \quad (23)$$

In the continuum limit $h \rightarrow 0$, we obviously have

$$D_1 = \frac{1}{3N^2} \int_0^{\infty} dt \left\langle \vec{A}(0) \cdot \vec{A}(t) \right\rangle, \quad (24)$$

where the previous formulae tell us how the integral should be consistently discretized. Concerning D_2 , one obtains

$$D_2 = \frac{1}{3N^2 h^{1/2}} \int_0^{\infty} dt \left\langle \vec{B}(0) \cdot \vec{A}(t) \right\rangle. \quad (25)$$

At first glance, this looks as if this contribution would diverge for $h \rightarrow 0$, but this is not the case. Rather, the correlation function $\left\langle \vec{B}(0) \cdot \vec{A}(t) \right\rangle$ depends on the time step, and is, to leading order, proportional to $h^{1/2}$, such that D_2 converges to a well-defined non-trivial value. This is demonstrated in Fig. 1, where $\left\langle \vec{B}(0) \cdot \vec{A}(t) \right\rangle h^{-1/2}$ is plotted for $N = 6$ and various time steps h . The $h^{1/2}$ dependence may be explained by linear response theory: As $\left\langle \vec{A} \right\rangle$ vanishes for symmetry reasons, only that part of \vec{A} will contribute to $\left\langle \vec{B}(0) \cdot \vec{A}(t) \right\rangle$ which is actually the response to the “kick” at time zero. This “kick”, however, has an infinitesimally small amplitude of order $h^{1/2}$. Therefore, linear response theory should be applicable, and the response in \vec{A} should be proportional to $h^{1/2}$ as well.

On a more formal level, we can write the Ermak–McCammion updating rule (Eq. 9) in the continuum limit as a Langevin equation with Ito interpretation:

$$\frac{d}{dt} \vec{r}_i = \sum_j \hat{\mu}_{ij} \cdot \vec{F}_j + \vec{f}_i, \quad (26)$$

where the noise term \vec{f}_i has zero mean, and variance

$$\left\langle \vec{f}_i(t) \otimes \vec{f}_j(t') \right\rangle = 2\vec{D}_{ij} \delta(t - t'), \quad (27)$$

i. e. \vec{f}_i corresponds to $\vec{\rho}_i/h$. This in turn implies $\vec{B} = h^{1/2} \sum_i \vec{f}_i$, such that D_2 can also be written as

$$D_2 = \frac{1}{3N^2} \sum_i \int_0^{\infty} dt \left\langle \vec{f}_i(0) \cdot \vec{A}(t) \right\rangle. \quad (28)$$

In seeming contrast to this result ($D = D^{(K)} + D_1 + D_2$), Fixman²⁴ rather obtained from linear response theory $D = D^{(K)} - D_1$, where D_1 is defined precisely as in Eq. 24. His result is however as valid as ours, and in what follows we will give an alternative derivation based on the Mori–Zwanzig projection operator formalism⁴². The

only conclusion is that D_1 and D_2 must satisfy the relation $D_2 = -2D_1$. Unfortunately, we have not been able to derive this result directly; however, it is very nicely borne out by our numerical data (Table I). Furthermore, if $\left\langle \vec{A}(0) \cdot \vec{A}(t) \right\rangle$ is positive for all times (as it is the case for our simulation data), it is immediately obvious that D must indeed be smaller than $D^{(K)}$.

For the Mori–Zwanzig analysis of D , we first notice that the Langevin equation corresponds to the Fokker–Planck equation (Kirkwood diffusion equation)

$$\frac{\partial}{\partial t} P(\Gamma, t | \Gamma^0, 0) = -i\mathcal{L}P(\Gamma, t | \Gamma^0, 0), \quad (29)$$

where Γ is a shorthand notation for the set of all monomer coordinates, $P(\Gamma, t | \Gamma^0, 0)$ is the transition probability density for the system going from Γ^0 at time 0 to Γ at time t , and $-i\mathcal{L}$ is the Fokker–Planck operator

$$-i\mathcal{L} = \sum_{ij} \frac{\partial}{\partial \vec{r}_i} \cdot \vec{D}_{ij} \cdot \left(\frac{\partial}{\partial \vec{r}_j} - \beta \vec{F}_j \right), \quad (30)$$

where $\beta = 1/(k_B T)$. The formal solution is $P = \exp(-i\mathcal{L}t)\delta(\Gamma - \Gamma^0)$, while the equilibrium distribution (i. e. the $t \rightarrow \infty$ solution) is

$$\rho(\Gamma) = \frac{\exp(-\beta U)}{\int d\Gamma \exp(-\beta U)}, \quad (31)$$

where U is the potential energy, such that $\vec{F}_i = -\partial U / \partial \vec{r}_i$, and

$$\rho \frac{\partial}{\partial \vec{r}_i} f = \left(\frac{\partial}{\partial \vec{r}_i} - \beta \vec{F}_i \right) \rho f \quad (32)$$

for an arbitrary function $f(\Gamma)$. Except for $-i\mathcal{L}$, we also need $i\mathcal{L}^\dagger$, which is the adjoint operator of $-i\mathcal{L}$ with respect to the standard scalar product $(f|g) = \int d\Gamma f(\Gamma)^* g(\Gamma)$ (f^* denoting the complex conjugate),

$$i\mathcal{L}^\dagger = \sum_{ij} \left(\frac{\partial}{\partial \vec{r}_j} + \beta \vec{F}_j \right) \cdot \vec{D}_{ij} \cdot \frac{\partial}{\partial \vec{r}_i}, \quad (33)$$

as well as $-i\hat{\mathcal{L}}$, which is the adjoint operator of $i\mathcal{L}^\dagger$ with respect to the natural scalar product

$$(f|g) = \int d\Gamma \rho(\Gamma) f(\Gamma)^* g(\Gamma). \quad (34)$$

From Eq. 32, and partial integration, one finds that $-i\hat{\mathcal{L}}$ coincides with $i\mathcal{L}^\dagger$.

We now use the standard memory equation as derived in Ref. 42. In Ref. 43 it was shown how to generalize this to the case of non-Hamiltonian dynamics; specifically it was shown there that the integral over the time correlation function of a slow variable S satisfies the relation

$$\int_0^\infty dt \langle S(0)^* S(t) \rangle = - \langle S|S \rangle^2 \times \left[\langle S|i\mathcal{L}^\dagger|S \rangle + \int_0^\infty dt \langle S|i\mathcal{L}^\dagger \mathcal{Q} \exp(i\mathcal{L}^\dagger t) \mathcal{Q} i\mathcal{L}^\dagger|S \rangle \right]^{-1}. \quad (35)$$

Here \mathcal{Q} is the operator which projects onto the orthogonal space of the slow variable, i. e. onto the space of variables which are (statically) uncorrelated with S . For the analysis of diffusion we study the variable

$$S = \exp(i\vec{q} \cdot \vec{R}_{CM}) \quad (36)$$

in the limit $q \rightarrow 0$ such that q^{-1} is much larger than the polymer gyration radius. Therefore,

$$\langle S(0)^* S(t) \rangle = \left\langle \exp \left[i\vec{q} \cdot (\vec{R}_{CM}(t) - \vec{R}_{CM}(0)) \right] \right\rangle. \quad (37)$$

For times of order of the Zimm relaxation time, or smaller, this correlation function is very close to unity, due to the smallness of q . For times much larger, the motion of \vec{R}_{CM} is just a Gaussian random walk with diffusion constant D , and hence

$$\begin{aligned} \langle S(0)^* S(t) \rangle &= \exp \left(-\frac{q^2}{6} \langle (\vec{R}_{CM}(t) - \vec{R}_{CM}(0))^2 \rangle \right) \\ &= \exp(-Dq^2 t). \end{aligned} \quad (38)$$

Thus the left hand side of Eq. 35 is just

$$\int_0^\infty dt \langle S(0)^* S(t) \rangle = \frac{1}{Dq^2}. \quad (39)$$

As $\langle S|S \rangle = 1$, we have

$$\begin{aligned} D &= -q^{-2} \langle S|i\mathcal{L}^\dagger|S \rangle \\ &= -q^{-2} \int_0^\infty dt \langle S|i\mathcal{L}^\dagger \mathcal{Q} \exp(i\mathcal{L}^\dagger t) \mathcal{Q} i\mathcal{L}^\dagger|S \rangle \end{aligned} \quad (40)$$

in the limit $q \rightarrow 0$. Now, straightforward evaluation yields

$$\begin{aligned} i\mathcal{L}^\dagger S &= \sum_{ij} \left(\frac{i\vec{q}}{N} + \beta \vec{F}_j \right) \cdot \overleftrightarrow{D}_{ij} \cdot \frac{i\vec{q}}{N} S \\ &= -\frac{q^2}{N^2} \sum_{ij} \hat{q} \cdot \overleftrightarrow{D}_{ij} \cdot \hat{q} S + \frac{iq}{N} \hat{q} \cdot \vec{A} S \end{aligned} \quad (41)$$

and, for $q \rightarrow 0$,

$$\langle S|i\mathcal{L}^\dagger|S \rangle = -\frac{q^2}{N^2} \sum_{ij} \frac{1}{3} \text{Tr} \langle \overleftrightarrow{D}_{ij} \rangle = -q^2 D^{(K)} \quad (42)$$

(the \vec{A} term vanishes upon averaging, for symmetry reasons). This also means that in the limit $q \rightarrow 0$ the variable $i\mathcal{L}^\dagger S$ becomes orthogonal to S , implying that in this limit we can ignore the operator \mathcal{Q} in Eq. 40. Furthermore, in the memory integral it is sufficient to just take the term linear in q for $i\mathcal{L}^\dagger S$ — any higher order would

not contribute to D in the limit $q \rightarrow 0$. In this order we find $i\mathcal{L}^\dagger S = i\vec{q} \cdot \vec{A}/N$. As $-i\hat{\mathcal{L}} = i\mathcal{L}^\dagger$, the memory term becomes

$$\begin{aligned} &\int_0^\infty dt \langle S|i\mathcal{L}^\dagger \mathcal{Q} \exp(i\mathcal{L}^\dagger t) \mathcal{Q} i\mathcal{L}^\dagger|S \rangle \\ &= \frac{q^2}{3N^2} \int_0^\infty dt \langle \vec{A}(0) \cdot \vec{A}(t) \rangle = q^2 D_1. \end{aligned} \quad (43)$$

Combining these results, we obtain Fixman's²⁴ formula $D = D^{(K)} - D_1$.

B. Numerical Results

As we have seen in the previous subsection, the relation $2D_1 + D_2 = 0$ should hold. Our data (see Table I) indeed confirm this prediction. Interestingly enough, we have found numerically that even the Green-Kubo integrands satisfy the corresponding relation

$$\Delta(t) \equiv 2 \langle \vec{A}(0) \cdot \vec{A}(t) \rangle + h^{-1/2} \langle \vec{B}(0) \cdot \vec{A}(t) \rangle = 0. \quad (44)$$

More precisely, we observed that for finite time step h there is a slight systematic deviation ($\Delta(t) \neq 0$), which however tends to zero for $h \rightarrow 0$. Furthermore, we found that $\Delta(t)$ quickly decays to zero with increasing time t , and has both a positive (small t) and a negative (larger t) contribution, such that $\int_0^\infty dt \Delta(t)$ is very small. Such discretization effects are the reason for our finding that the two functions

$$D(t) \equiv D^{(K)} + D_1(t) + D_2(t) \quad (45)$$

and

$$\tilde{D}(t) \equiv D^{(K)} - D_1(t), \quad (46)$$

with

$$D_1(t) = \frac{1}{3N^2} \int_0^t d\tau \langle \vec{A}(0) \cdot \vec{A}(\tau) \rangle \quad (47)$$

and

$$D_2(t) = \frac{1}{3N^2 h^{1/2}} \int_0^t d\tau \langle \vec{B}(0) \cdot \vec{A}(\tau) \rangle, \quad (48)$$

are slightly different, in particular for short times. This is seen in Fig. 2, which shows $D(t)$ and $\tilde{D}(t)$ for $N = 6, 25, \text{ and } 50$, as a function of $1/t$, with logarithmic abscissa. This figure also demonstrates that our data are well-converged and accurate enough to clearly discriminate between short- and long-time regimes.

Table I summarizes our results for the diffusion coefficient, where we list $D^{(K)}$, D_1 and D_2 . The data confirm the relation $2D_1 + D_2 = 0$ within our error bars up to $N = 50$. As it turned out that D_2 is much harder to sample than D_1 , we did not test the relation for the

longer chains $N = 100$ and 200 , where our statistics is not sufficient. The data also show that the relative contribution of the correction term systematically increases with chain length (roughly 1% for $N = 6$, roughly 3.5% for $N = 200$).

Comparing our values for $D^{(K)}$ and D_1 with those of Ref. 31, we see that they are compatible within error bars. However, Rey *et al.*³¹ have obtained values for D which are larger than $D^{(K)}$. In view of this puzzle, we have done a test run for $N = 6$, where we increased the time step to their value $h = 0.01$, and decreased the observation time to theirs (0.2×10^6 time steps). Figure 3 shows our results for $D_1(t)$ and $D_2(t)$. One sees that the statistical accuracy is sufficient to obtain an acceptable value for D_1 , but that it is by far not enough to estimate D_2 . We believe that this is the most likely explanation for the deviations observed in Ref. 31.

IV. SCALING OF THE $\langle AA \rangle$ CORRELATION FUNCTION

The systematic increase of the ratio $D_1/D^{(K)}$ with chain length, as seen from the data in Table I, raises the question if that ratio will saturate at a finite value, or keep on increasing, or maybe even tend to zero for $N \rightarrow \infty$, after going through a maximum. We cannot give a conclusive answer to this question; however, we have found some interesting results concerning the issue. Rewriting the Green–Kubo formula for D_1 as

$$D_1 = \frac{\langle A^2 \rangle}{3N^2} \int_0^\infty dt C_A(t), \quad (49)$$

where C_A is the normalized A – A autocorrelation function,

$$C_A(t) = \frac{1}{\langle A^2 \rangle} \langle \vec{A}(0) \cdot \vec{A}(t) \rangle, \quad (50)$$

one sees that the N dependence is clear if it is known for $\langle A^2 \rangle$ and for $\tau_A = \int_0^\infty dt C_A(t)$. As $\langle A^2 \rangle$ is a static average, let us discuss it first.

For *fluctuating* hydrodynamic interactions, we notice that $\sum_j \vec{\mu}_{ij} \cdot \vec{F}_j$ is nothing but the velocity flow field generated at position of monomer i , due to all the forces acting on the other monomers j . However, the system is in thermal equilibrium. Therefore, one should expect that this velocity is of order of a typical thermal velocity. Furthermore, in equilibrium the flow velocities at different volume elements are statistically uncorrelated. This picture suggests that \vec{A} is essentially the sum of N statistically independent random variables, each of which *does not* depend on N . Therefore, the scaling

$$\langle A^2 \rangle \propto N \quad (51)$$

is expected from standard statistics, and this argument should be true independently of the details of the chain conformations.

For *preaveraged* hydrodynamic interactions, however, this argument does *not* hold (the preaveraging prevents $\vec{\mu}_{ij}$ from “thermalizing”). Here we rather write

$$\langle A^2 \rangle = \sum_{ij} \sum_{kl} \langle \mu_{ij}^{\alpha\beta} \rangle \langle \mu_{kl}^{\alpha\gamma} \rangle \langle F_j^\beta F_l^\gamma \rangle, \quad (52)$$

where summation over repeated Cartesian indices, denoted by the Greek letters, is implied. Exploiting the isotropy of the $\langle \vec{F} \otimes \vec{F} \rangle$ tensor (i. e. its proportionality to the unit tensor) one finds

$$\langle A^2 \rangle = \frac{1}{3} \sum_{ij} \sum_{kl} \langle \mu_{ij}^{\alpha\beta} \rangle \langle \mu_{kl}^{\alpha\beta} \rangle \langle \vec{F}_j \cdot \vec{F}_l \rangle. \quad (53)$$

This is simple to study for the case of a *Gaussian* chain, since then the $\langle \vec{F} \cdot \vec{F} \rangle$ correlation is strictly short-ranged. Indeed, for a random-walk chain, $\langle \vec{F}_i \cdot \vec{F}_j \rangle$ must be zero if i and j are sufficiently far away from each other, since in that case one can choose a “pivot” monomer between i and j , and rotate the “right” part of the chain around that monomer by a random angle, without changing the statistical weight of the conformation. If j is on the rotated part, \vec{F}_j is changed, while \vec{F}_i is unchanged. Thus one shows $\langle \vec{F}_i \cdot \vec{F}_j \rangle = -\langle \vec{F}_i \cdot \vec{F}_j \rangle = 0$. This argument holds whenever it is possible to find a pivot monomer, i. e. for $|i - j| \geq 2$. Thus the only remaining correlations are those for $i = j$ and $|i - j| = 1$, in which case the correlation is obvious, due to the spring interaction with the neighboring monomer. In case of an excluded-volume chain we rather expect a power-law decay⁴⁴, related to the probability of loops of length $|i - j|$. In what follows, we will therefore, for simplicity, focus on the Gaussian case. Noticing $\langle \vec{\mu}_{ij} \rangle \propto |i - j|^{-1/2}$, we thus find

$$\langle A^2 \rangle \propto \int_0^N dx \int_0^N dy \int_0^N dz |x - y|^{-1/2} |z - y|^{-1/2} \quad (54)$$

(the short range of $\langle \vec{F} \cdot \vec{F} \rangle$ reduces the number of integrations from four to three). A trivial transformation to reduced variables x/N etc. then shows

$$\langle A^2 \rangle \propto N^2 \quad (55)$$

for preaveraged hydrodynamics in the Gaussian case.

We have tested these predictions numerically, and exploited the fact that $\langle A^2 \rangle$ is a static average, and, as such, amenable to efficient Monte Carlo procedures. This is particularly true for the Gaussian case, where one simply generates a sample of chains. We were therefore able to study this case up to chains of length $N = 0.8 \times 10^5$. However, we restricted ourselves, for simplicity, to Oseen-like hydrodynamic interactions, where we studied both the

fluctuating and the preaveraged case. Apart from this, we also studied the behavior for our model (fluctuating hydrodynamics, excluded-volume chains) up to chains of length $N = 10^4$. In this case, we used the full RPY interaction, and generated the conformations by a combination of the pivot algorithm^{40,41} with local moves. For every chain length, 0.2×10^5 pivot moves, and 100 times as many local moves, were used. The results are presented in Fig. 4; indeed reasonable agreement with our predictions is found.

The scaling laws for $\langle A^2 \rangle$ have an interesting implication for the dynamics of \vec{A} . Writing $\langle A^2 \rangle \propto N^x$ where $x = 1, 2$ for the discussed cases, and $\tau_A \propto N^y$, we find from Eq. 49

$$D_1 \propto N^{x+y-2}. \quad (56)$$

On the other hand, it is well-established that $D^{(K)}$ is proportional to $N^{-\nu}$ where ν is 1/2 for Gaussian chains, and 0.59 for excluded-volume chains. It also strongly believed that this is the asymptotic scaling law for D . This, however, implies that D_1 must decay sufficiently quickly as a function of N — otherwise D_1 would ultimately dominate and spoil the scaling of D . More precisely, one expects $D_1 \propto N^{-\phi}$ with $\phi \geq \nu$. Combined with the previous consideration, this yields $\phi = 2 - x - y \geq \nu$ or $y \leq 2 - x - \nu$, i. e. $y \leq 1 - \nu$ for fluctuating hydrodynamics, and $y \leq -\nu$ for preaveraged hydrodynamics of a Gaussian chain. This is a quite counter-intuitive result, since it implies that τ_A would increase only very weakly with chain length for fluctuating hydrodynamics, while it would even *decrease* for preaveraged hydrodynamics! Naively, one would rather expect that \vec{A} , as a collective quantity, decays on the same time scale as the overall polymer conformations, i. e. $\tau_A \propto \tau_Z \propto N^{3\nu}$ (this latter relation is the standard Zimm scaling law¹¹, and implies a rather sharp increase with N). We have thus found a “collective” quantity which apparently decays much more rapidly than the chain as a whole. We believe this issue deserves further attention; in particular, we think it would be very desirable to try to understand the underlying physical mechanisms governing the relaxation of \vec{A} somewhat better.

Our numerical data from the BD simulation (i. e. for fluctuating hydrodynamics, and excluded-volume chains) can only give us very limited hints on the behavior of τ_A as a function of N , since, due to the overall computational demand, we were not able to simulate the dynamics with sufficient accuracy for chains longer than $N = 200$. Our data for $C_A(t)$ are presented in Fig. 5. Apparently the correlation function has two distinct time regimes. In the short-time regime ($t < t_0$), the curves are practically superimposable. This is similar to the observations made by Fixman²⁶. In the long-time regime ($t > t_0$), the correlation functions decay exponentially with a correlation time τ_D , $C_A(t) \propto \exp(-t/\tau_D)$. Figure 6 shows our data for τ_D . Indeed τ_D increases with chain length; however, the observed behavior in our limited N

window is anything but a power law. According to our previous considerations, the increase of τ_D should not be stronger than $N^{1-\nu}$. Indeed this condition seems to be satisfied in the regime of longer chains.

V. FURTHER RESULTS

A. Static Scaling Properties

The radius of gyration and end-to-end distance are given by

$$\langle R_g^2 \rangle = \frac{1}{2N^2} \sum_{ij} \langle r_{ij}^2 \rangle \quad (57)$$

and

$$\langle R_e^2 \rangle = \langle (\vec{r}_N - \vec{r}_1)^2 \rangle. \quad (58)$$

The theoretical scaling for these static properties is

$$\langle R_g^2 \rangle \propto \langle R_e^2 \rangle \propto (N-1)^{2\nu}. \quad (59)$$

In good solvent, the scaling exponent has the theoretical value of $\nu \approx 0.588$ from renormalization group calculations and Monte Carlo simulations⁴⁵. The log-log fits of $\langle R_e^2 \rangle$ and $\langle R_g^2 \rangle$ vs. $N-1$ yield the exponents $2\nu = 1.187 \pm 0.003$ and $2\nu = 1.133 \pm 0.006$, respectively (see Fig. 7), which is similar to the results by Rey *et al.*³¹.

Similarly, the static structure factor

$$\begin{aligned} S(k) &= \frac{1}{N} \sum_{ij} \langle \exp(i\vec{k} \cdot \vec{r}_{ij}) \rangle \\ &= \frac{1}{N} \sum_{ij} \left\langle \frac{\sin(kr_{ij})}{kr_{ij}} \right\rangle, \end{aligned} \quad (60)$$

which is measured in scattering experiments, obeys the scaling relation

$$S(k) \propto k^{-1/\nu} \quad (61)$$

in the regime $R_g^{-1} \ll k \ll b^{-1}$. By fitting a power law to our data we get the value (see Fig. 8) $\nu = 0.575 \pm 0.004$.

We have also obtained the first cumulant (or initial decay rate), $\Omega(k)$, of the dynamic structure factor $S(k, t)$, defined as

$$\Omega(k) = -\lim_{t \rightarrow 0} \frac{d}{dt} \left(\frac{S(k, t)}{S(k, 0)} \right). \quad (62)$$

Akcasu *et al.*^{12,46} have shown that $\Omega(k)$ can be written as

$$\Omega(k) = \frac{\sum_{ij} \langle \vec{k} \cdot \vec{D}_{ij} \cdot \vec{k} \exp(i\vec{k} \cdot \vec{r}_{ij}) \rangle}{\sum_{ij} \langle \exp(i\vec{k} \cdot \vec{r}_{ij}) \rangle}. \quad (63)$$

The orientational averaging in Eq. (63) is easily done for the RPY tensor^{31,47}. For the denominator one obtains

$$\left\langle \exp(i\vec{k} \cdot \vec{r}_{ij}) \right\rangle_{or} = \frac{\sin z}{z} \quad (64)$$

with $z = kr_{ij}$. In the numerator we find for $i = j$

$$\left\langle (\vec{k} \cdot \overleftrightarrow{D}_{ij} \cdot \vec{k}) \exp(i\vec{k} \cdot \vec{r}_{ij}) \right\rangle_{or} = \frac{k_B T}{6\pi\eta a} k^2. \quad (65)$$

For $i \neq j$ one obtains instead

$$\begin{aligned} & \left\langle (\vec{k} \cdot \overleftrightarrow{D}_{ij} \cdot \vec{k}) \exp(i\vec{k} \cdot \vec{r}_{ij}) \right\rangle_{or} \\ &= \frac{k_B T}{4\pi\eta r_{ij}} k^2 \left[\left(1 - \frac{2}{3} \frac{a^2}{r_{ij}^2} \right) \frac{\sin z}{z} \right. \\ & \quad \left. + \left(1 - 2 \frac{a^2}{r_{ij}^2} \right) \left(\frac{\cos z}{z^2} - \frac{\sin z}{z^3} \right) \right] \end{aligned} \quad (66)$$

in the case of large distances $r_{ij} \geq 2a$, while

$$\begin{aligned} & \left\langle (\vec{k} \cdot \overleftrightarrow{D}_{ij} \cdot \vec{k}) \exp(i\vec{k} \cdot \vec{r}_{ij}) \right\rangle_{or} \\ &= \frac{k_B T}{6\pi\eta a} k^2 \left[\left(1 - \frac{3}{16} \frac{r_{ij}}{a} \right) \frac{\sin z}{z} \right. \\ & \quad \left. + \frac{3}{16} \frac{r_{ij}}{a} \left(\frac{\cos z}{z^2} - \frac{\sin z}{z^3} \right) \right] \end{aligned} \quad (67)$$

for $r_{ij} < 2a$. We should mention that there are some typographical errors both in Ref. 31 and Ref. 47. The right-hand term of Eq. (63) is therefore directly calculated from the trajectories. In the $k \rightarrow 0$ limit, $\Omega(k)$ reflects exclusively the translational motion contribution to the chain dynamics. Therefore, the Kirkwood formula can be recovered from the first cumulant as

$$D^{(K)} = \lim_{k \rightarrow 0} \Omega(k)/k^2. \quad (68)$$

We have obtained $D^{(K)}$ through Eq. (68) from the intercept of a fitting of $\Omega(k)/k^2$ vs. k in the $k \rightarrow 0$ limit shown in Fig. 9. These values are exactly the same as those obtained from Eq. (4), which constitutes a further verification of the consistency of our numerical method. From Fig. 9, a universal dependence of the type $\Omega(k)/k^2 \propto k$ is also obtained in the scaling regime $R_g^{-1} \ll k \ll b^{-1}$.

B. Dynamic Scaling Properties

An approximately exponential behavior of the time-correlation function $\left\langle \vec{R}_e(t) \cdot \vec{R}_e(0) \right\rangle$, where \vec{R}_e is the end-to-end vector, is observed (see Fig. 10). We have extracted the relaxation times (Zimm times) τ_Z corresponding to this behavior. τ_Z is related to the orientational diffusion of the end-to-end vector. A log-log fit

of τ_Z vs. N yields a slope of 1.71 ± 0.01 (Fig. 11), which is close to the theoretical value 3ν with hydrodynamic interactions.

The dynamic structure factor

$$S(k, t) = \frac{1}{N} \sum_{ij} \left\langle \exp \left[i\vec{k} \cdot (\vec{r}_i(t) - \vec{r}_j(0)) \right] \right\rangle \quad (69)$$

is predicted to exhibit scaling behavior¹¹ if both wave number and time are in the scaling regime, i. e. $R_g^{-1} \ll k \ll b^{-1}$ and $\tau_0 \ll t \ll \tau_Z$, where τ_0 is the microscopic time and τ_Z is the Zimm time, the longest relaxation time of the chain. Fig. 12 gives a nice data collapse for the expected form

$$\frac{S(k, t)}{S(k, 0)} = f \left(k^2 t^{2/3} \right) \quad (70)$$

in log-linear representation.

These scaling results demonstrate the internal consistency of our simulation, and in all cases agreement with the pertinent theories and experimental results.

VI. SUMMARY

The present study has shown that Brownian Dynamics simulations are able to attack the problem of translational diffusion of polymer chains with hydrodynamic interaction and excluded volume. It has also highlighted the necessity of substantial statistical effort in order to obtain reliable data. While the standard picture of static and dynamic scaling is reproduced, as in previous studies, the novel aspect is the calculation of the diffusion coefficient to sufficiently high accuracy, such that the difference between the short-time Kirkwood value and the asymptotic long-time value could be resolved unambiguously. The numerical data are in perfect agreement with the theoretical predictions, both concerning the short-time value, and the crossover to the long-time value described by Fixman's Green-Kubo formula. It turns out that the long-time value is a few percent less than the short-time value. For Fixman's Green-Kubo integrand we find two remarkable results, namely that its initial value behaves very differently for preaveraged vs. fluctuating hydrodynamics, and that the correlation function, though describing a global property of the chain, must decay substantially faster than the conformations, in order to avoid a violation of dynamic scaling. Our numerical data are in reasonable agreement with these considerations, but not fully conclusive since only short chains were accessible. More work on this issue, in particular aimed at a better physical understanding, is clearly desirable.

- ¹ J. G. Kirkwood and J. Riseman, *J. Chem. Phys.* **16**, 565 (1948).
- ² J. G. Kirkwood, *J. Polym. Sci.* **12**, 1 (1953).
- ³ Y. Ikeda, *Kobayashi Rigaku Kenkyusho Hokoku* **6**, 44 (1956).
- ⁴ B. H. Zimm, *J. Chem. Phys.* **24**, 269 (1956).
- ⁵ J. Erpenbeck and J. G. Kirkwood, *J. Chem. Phys.* **29**, 909 (1963).
- ⁶ M. Fixman, *J. Chem. Phys.* **42**, 3831 (1965).
- ⁷ C. W. Pyun and M. Fixman, *J. Chem. Phys.* **42**, 3838 (1965).
- ⁸ A. Horta and M. Fixman, *J. Am. Chem. Soc.* **90**, 3048 (1968).
- ⁹ B. H. Zimm, *Macromolecules* **13**, 592 (1980).
- ¹⁰ G. Wilemski and G. Tanaka, *Macromolecules* **14**, 1531 (1981).
- ¹¹ M. Doi and S. F. Edwards, *The Theory of Polymer Dynamics*, Clarendon Press, Oxford, 1986.
- ¹² A. Z. Akcasu, M. Benmouna, and C. C. Han, *Polymer* **21**, 866 (1980).
- ¹³ C. C. Han and A. Z. Akcasu, *Macromolecules* **14**, 1080 (1981).
- ¹⁴ Y. Tsunashima, M. Hirata, N. Nemoto, and M. Kurata, *Macromolecules* **20**, 1992 (1987).
- ¹⁵ M. Bhatt, A. M. Jamieson, and R. G. Petschek, *Macromolecules* **22**, 1374 (1989).
- ¹⁶ C. Pierleoni and J. P. Ryckaert, *J. Chem. Phys.* **96**, 8539 (1992).
- ¹⁷ B. Dünweg and K. Kremer, *J. Chem. Phys.* **99**, 6983 (1993).
- ¹⁸ J. P. Hansen and I. R. McDonald, *Theory of Simple Liquids*, Academic, New York, 1986.
- ¹⁹ A. Kopf, B. Dünweg, and W. Paul, *J. Chem. Phys.* **107**, 6945 (1997).
- ²⁰ P. Ahrlich and B. Dünweg, *J. Chem. Phys.* **111**, 8225 (1999).
- ²¹ H. C. Öttinger, *J. Chem. Phys.* **87**, 3156 (1987).
- ²² J. Rotne and S. Prager, *J. Chem. Phys.* **50**, 4831 (1969).
- ²³ M. Fixman, *J. Chem. Phys.* **78**, 1588 (1983).
- ²⁴ M. Fixman, *Macromolecules* **14**, 1710 (1981).
- ²⁵ D. L. Ermak and J. A. McCammon, *J. Chem. Phys.* **69**, 1352 (1978).
- ²⁶ M. Fixman, *J. Chem. Phys.* **78**, 1594 (1983).
- ²⁷ M. Fixman, *Macromolecules* **19**, 1195 (1986).
- ²⁸ R. J. Lewis, S. A. Allison, D. Eden, and R. Pecora, *J. Chem. Phys.* **89**, 2490 (1988).
- ²⁹ W. Zylka and H. C. Öttinger, *J. Chem. Phys.* **90**, 474 (1989).
- ³⁰ A. Rey, J. J. Freire, and J. G. de la Torre, *J. Chem. Phys.* **90**, 2035 (1989).
- ³¹ A. Rey, J. J. Freire, and J. G. de la Torre, *Macromolecules* **24**, 4666 (1991).
- ³² A. Rey, J. J. Freire, and J. G. de la Torre, *Polymer* **33**, 3477 (1992).
- ³³ H. C. Öttinger, *Macromolecules* **27**, 3415 (1994).
- ³⁴ H. C. Öttinger, *Phys. Rev. E* **50**, 2696 (1994).
- ³⁵ A. V. Lyulin, D. B. Adolf, and G. R. Davies, *J. Chem. Phys.* **111**, 758 (1999).
- ³⁶ R. M. Jendrejack, M. D. Graham, and J. J. de Pablo, *J. Chem. Phys.* **113**, 4767 (2000).
- ³⁷ H. Yamakawa, *J. Chem. Phys.* **53**, 436 (1970).
- ³⁸ B. Dünweg and W. Paul, *Int. J. Mod. Phys. C* **2**, 817 (1991).
- ³⁹ H. Flyvbjerg and H. G. Petersen, *J. Chem. Phys.* **91**, 461 (1989).
- ⁴⁰ M. Lal, *Mol. Phys.* **17**, 57 (1969).
- ⁴¹ S. D. Stellman and P. J. Gans, *Macromolecules* **5**, 516 (1972).
- ⁴² D. Forster, *Hydrodynamic Fluctuations, Broken Symmetries, and Correlation Functions*, Benjamin-Cummings, London, 1983.
- ⁴³ B. Dünweg, *J. Chem. Phys.* **99**, 6977 (1993).
- ⁴⁴ P.-G. de Gennes, *Scaling Concepts in Polymer Physics*, Cornell University Press, Ithaca, 1979.
- ⁴⁵ B. Li, N. Madras, and A. D. Sokal, *J. Stat. Phys.* **80**, 661 (1995).
- ⁴⁶ M. Benmouna and A. Z. Akcasu, *Macromolecules* **13**, 409 (1980).
- ⁴⁷ W. Burchard, M. Schmidt, and W. H. Stockmayer, *Macromolecules* **13**, 580 (1980).

N	$D^{(K)}$	D_1	D_2	$2D_1 + D_2$	$ D_1 + D_2 /D^{(K)}$
6	0.3544 ± 10^{-4}	0.00408 ± 10^{-5}	-0.0081 ± 10^{-4}	0.0000 ± 10^{-4}	$0.0113 \pm 3 \times 10^{-4}$
8	0.3011 ± 10^{-4}	0.00441 ± 10^{-5}	-0.0087 ± 10^{-4}	0.0001 ± 10^{-4}	$0.0143 \pm 3 \times 10^{-4}$
11	0.2513 ± 10^{-4}	0.00450 ± 10^{-5}	-0.0089 ± 10^{-4}	0.0001 ± 10^{-4}	$0.0175 \pm 4 \times 10^{-4}$
15	0.2106 ± 10^{-4}	0.00443 ± 10^{-5}	-0.0088 ± 10^{-4}	0.0000 ± 10^{-4}	$0.0214 \pm 5 \times 10^{-4}$
20	0.1788 ± 10^{-4}	0.00443 ± 10^{-5}	-0.0084 ± 10^{-4}	0.0001 ± 10^{-4}	$0.0234 \pm 6 \times 10^{-4}$
25	0.1573 ± 10^{-4}	0.00422 ± 10^{-5}	-0.0079 ± 10^{-4}	0.0000 ± 10^{-4}	$0.0249 \pm 6 \times 10^{-4}$
30	0.1416 ± 10^{-4}	0.00399 ± 10^{-5}	-0.0076 ± 10^{-4}	0.0001 ± 10^{-4}	$0.0267 \pm 7 \times 10^{-4}$
35	0.1298 ± 10^{-4}	0.00381 ± 10^{-5}	-0.0072 ± 10^{-4}	0.0000 ± 10^{-4}	$0.0275 \pm 8 \times 10^{-4}$
40	0.1201 ± 10^{-4}	0.00363 ± 10^{-5}	-0.0069 ± 10^{-4}	0.0000 ± 10^{-4}	$0.0287 \pm 8 \times 10^{-4}$
45	0.1123 ± 10^{-4}	0.00345 ± 10^{-5}	-0.0066 ± 10^{-4}	0.0000 ± 10^{-4}	$0.0292 \pm 9 \times 10^{-4}$
50	0.1055 ± 10^{-4}	0.00332 ± 10^{-5}	-0.0063 ± 10^{-4}	0.0000 ± 10^{-4}	$0.0298 \pm 9 \times 10^{-4}$
100	0.0718 ± 10^{-4}	0.0022 ± 10^{-4}			$0.031 \pm 1 \times 10^{-3}$
200	0.0428 ± 10^{-4}	0.0015 ± 10^{-4}			$0.035 \pm 1 \times 10^{-3}$

TABLE I. The diffusion coefficients $D^{(K)}$, D_1 , D_2 , as well as $2D_1 + D_2$, and $|D_1 + D_2|/D^{(K)}$, as defined in the text, for different chain lengths N . Note that D_2 was not sampled for $N = 100$ and 200 , for reasons of poor statistics, and that hence for these chains we have assumed $|D_1 + D_2| = D_1$.

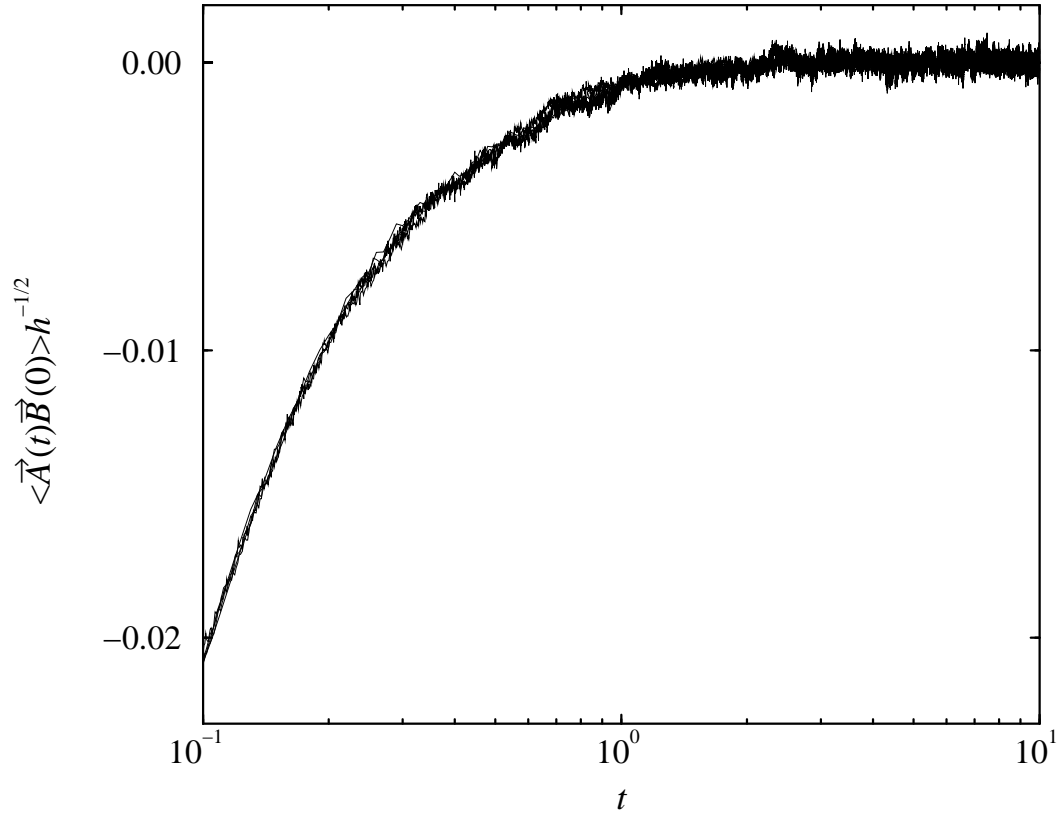


FIG. 1. The correlation function $\langle \vec{A}(t) \cdot \vec{B}(0) \rangle$, scaled with $h^{-1/2}$, for $N = 6$ and various time steps $h = 0.0005, 0.001, 0.002, 0.005$ and 0.01 , respectively.

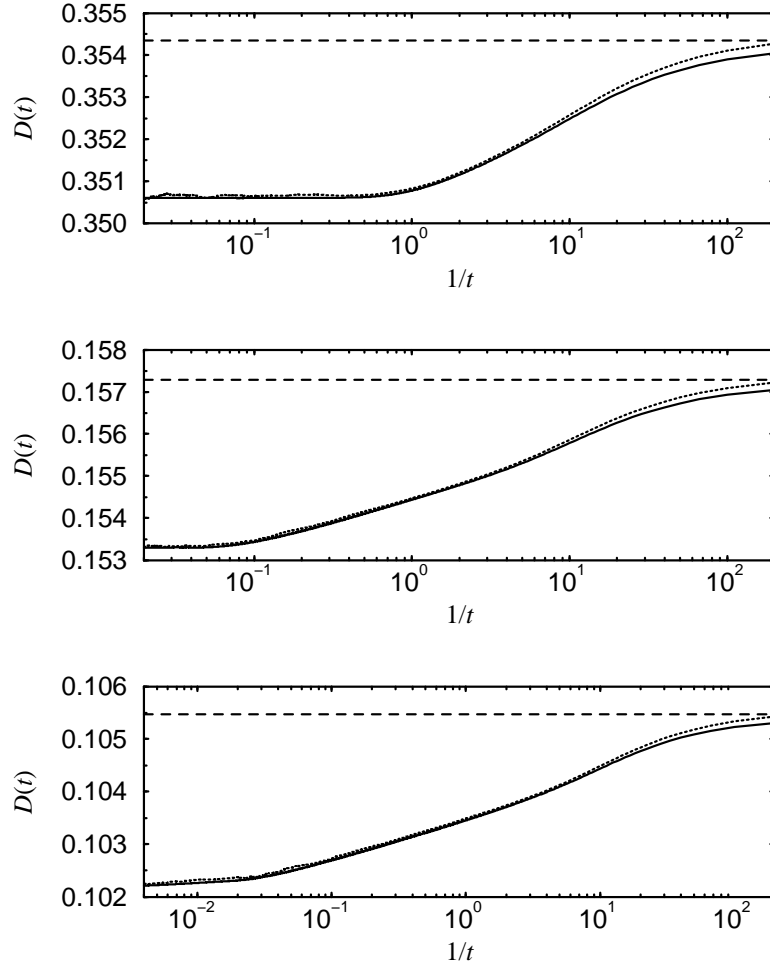


FIG. 2. Time-dependent diffusion coefficients $D(t) = D^{(K)} + D_1(t) + D_2(t)$ (dotted lines) and $\tilde{D}(t) = D^{(K)} - D_1(t)$ (full lines; see also Eq. 45 etc.), for $N = 6$ (upper graph), $N = 25$ (middle graph) and $N = 50$ (lower graph). The dashed lines indicate the corresponding Kirkwood values $D^{(K)}$.

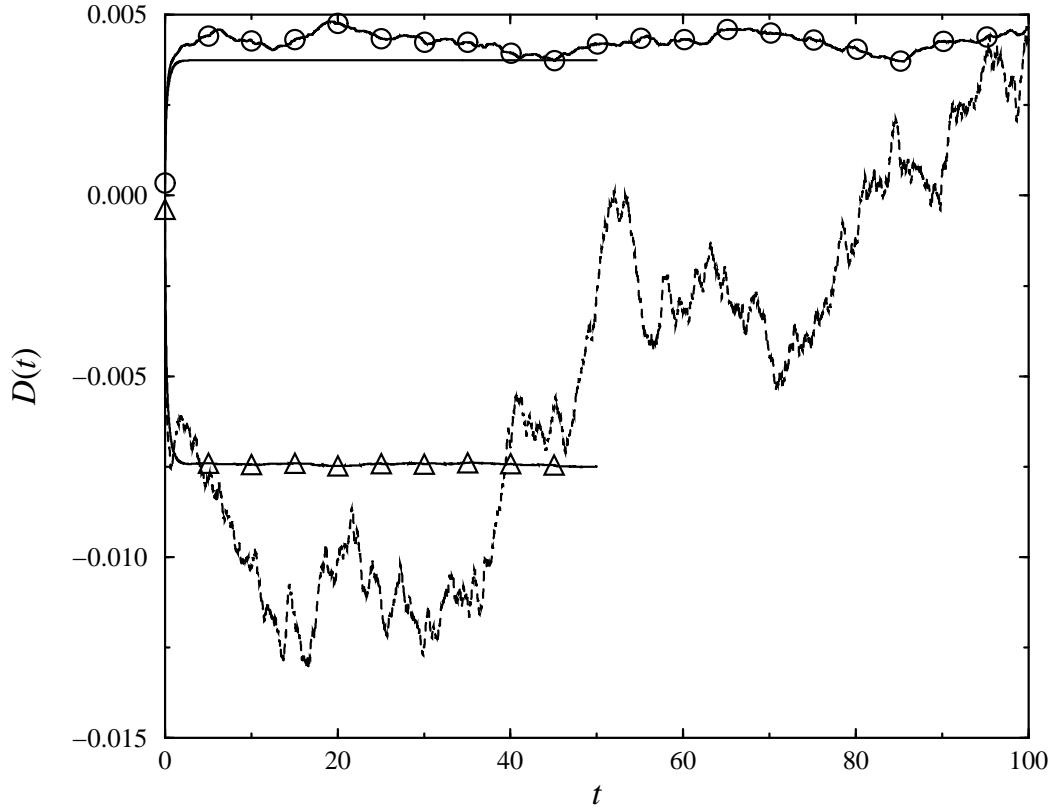


FIG. 3. Time-dependent diffusion coefficients $D_1(t)$ and $D_2(t)$ for $N = 6$ for different overall observation times: (i) Solid line: $D_1(t)$ (high resolution). (ii) Solid line with triangles: $D_2(t)$ (high resolution). (iii) Solid line with circles: $D_1(t)$ (low resolution). (iv) Dashed line: $D_2(t)$ (low resolution). The parameters of the low-resolution calculation are adapted to those of Rey *et al.*³¹, as explained in the text.

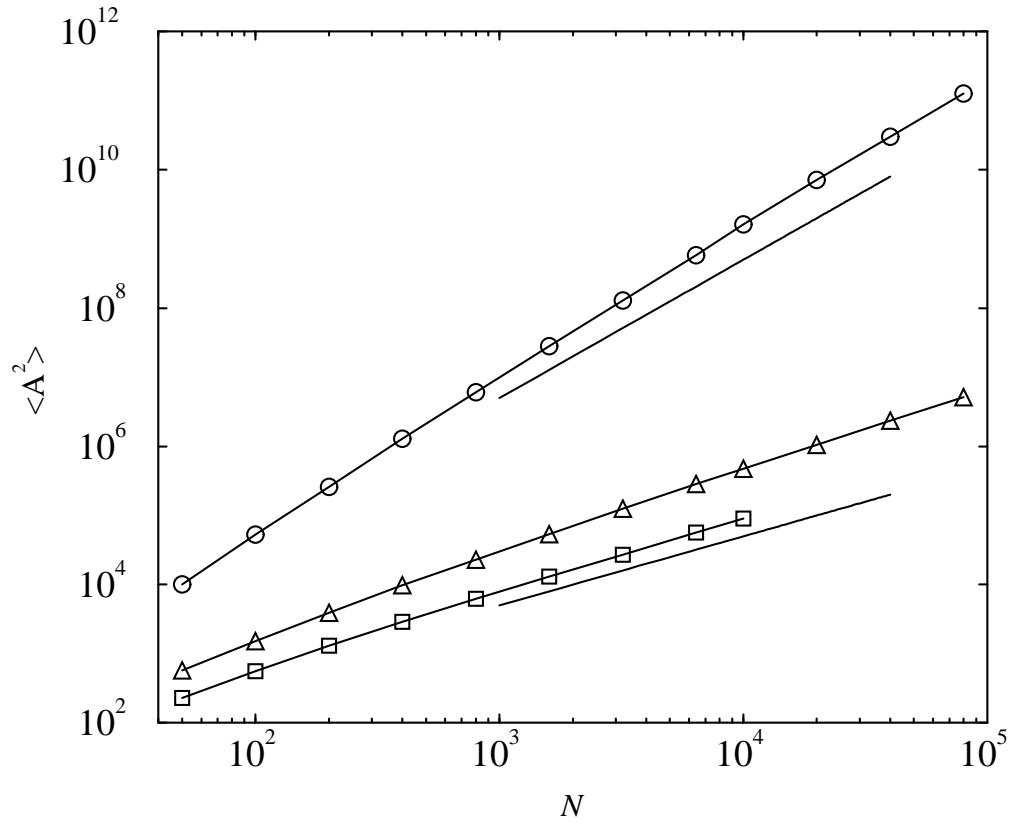


FIG. 4. Static average $\langle A^2 \rangle$ as a function of chain length N for different cases: (i) Gaussian chain with preaveraged hydrodynamics (circles); (ii) Gaussian chain with fluctuating hydrodynamics (triangles); (iii) excluded-volume chain with fluctuating hydrodynamics (squares). The slopes of the solid lines indicate the power laws N^2 and N^1 .

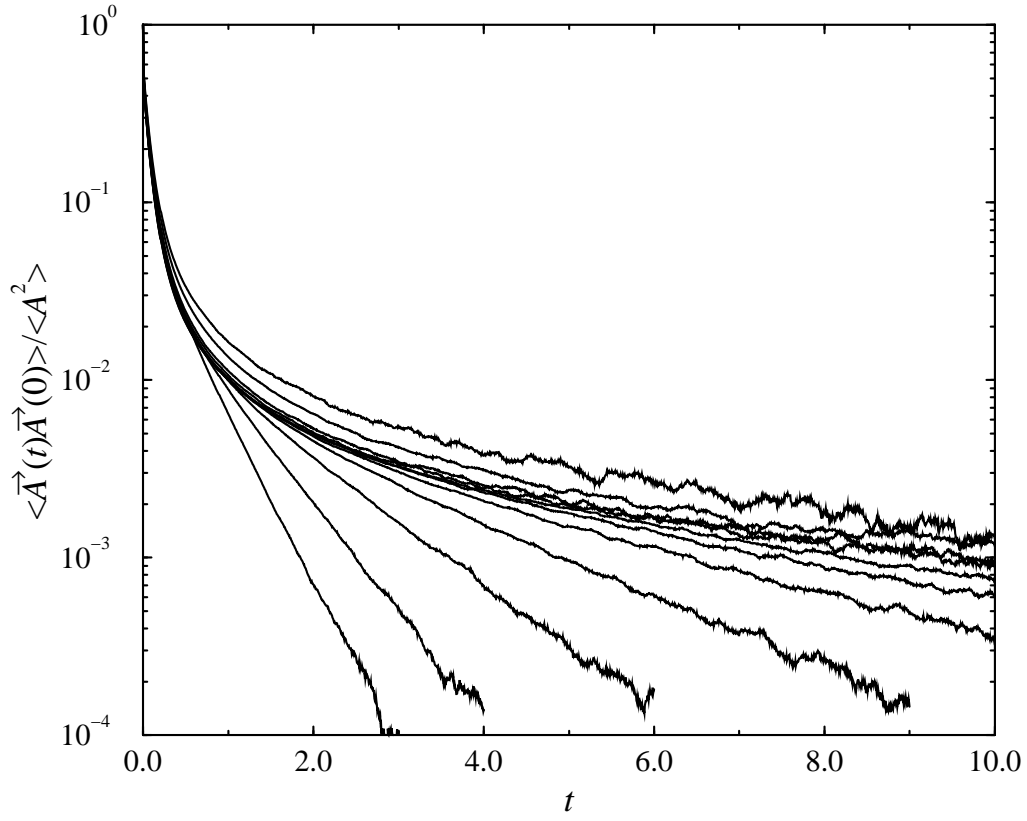


FIG. 5. Normalized autocorrelation function $\langle \vec{A}(t)\vec{A}(0) \rangle / \langle \vec{A}^2 \rangle$, for $N = 6, 8, 11, 15, 20, 25, 30, 40, 50, 100, 200$. The chain length increases from left to right.

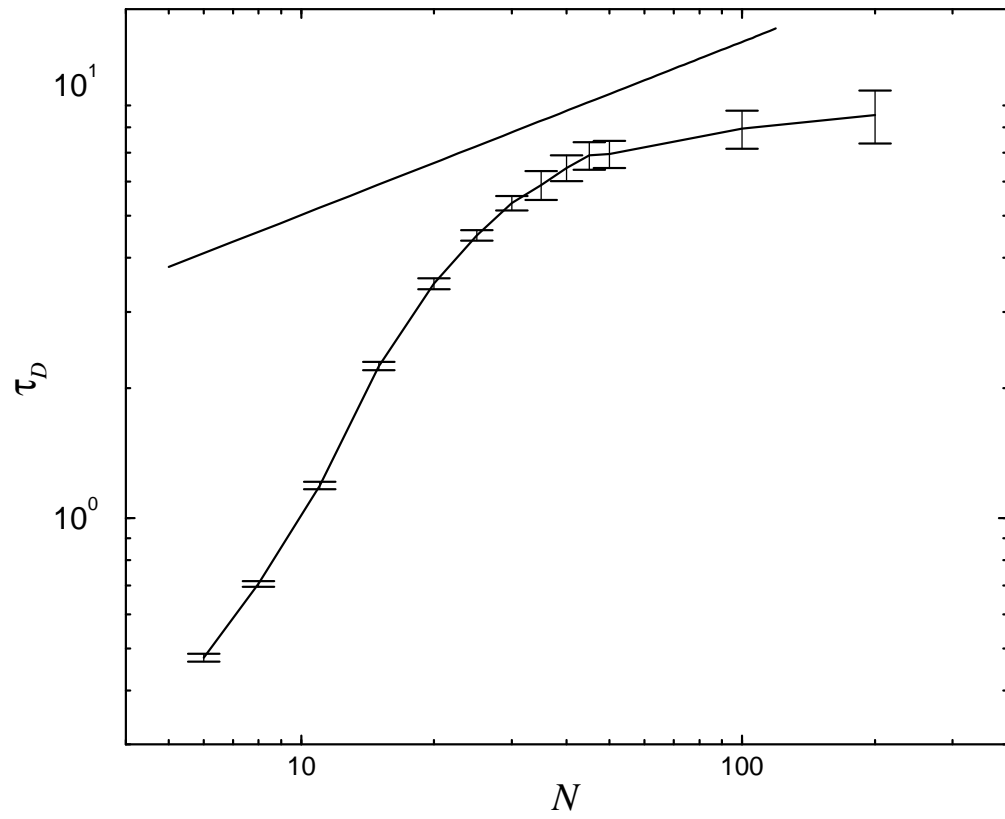


FIG. 6. Chain length scaling for τ_D . The slope of the solid line indicates the power law $N^{1-\nu}$.

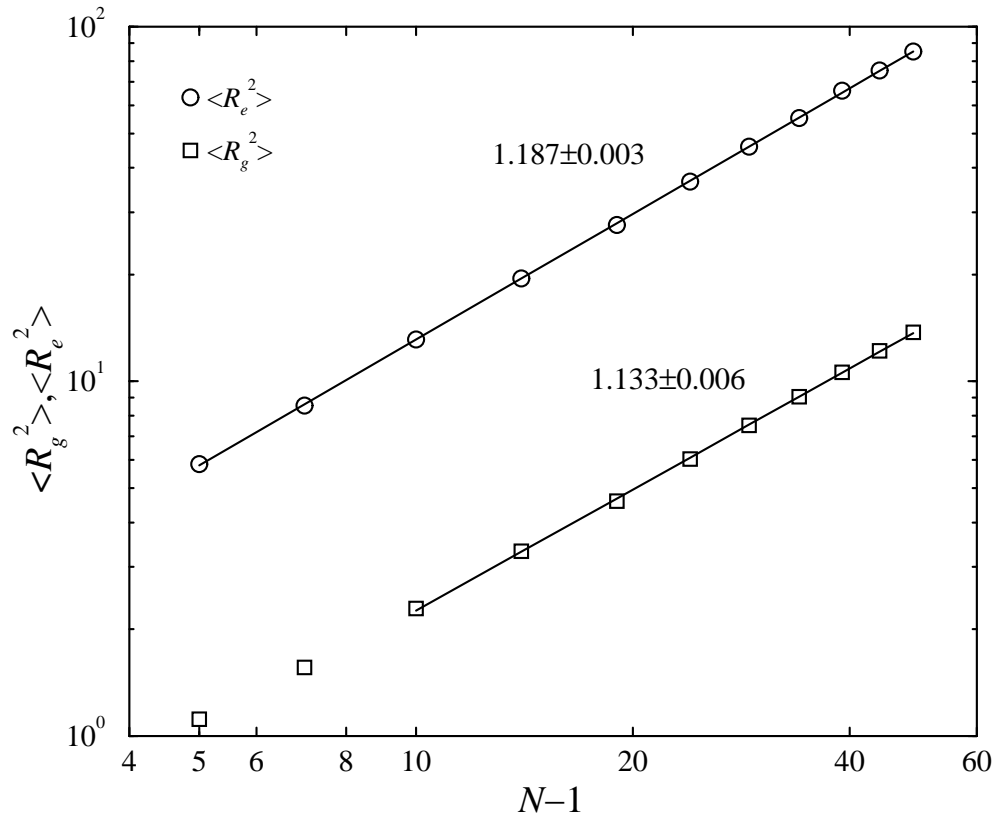


FIG. 7. Chain length scaling for $\langle R_g^2 \rangle$ and $\langle R_e^2 \rangle$. The error bars are smaller than the symbol size.

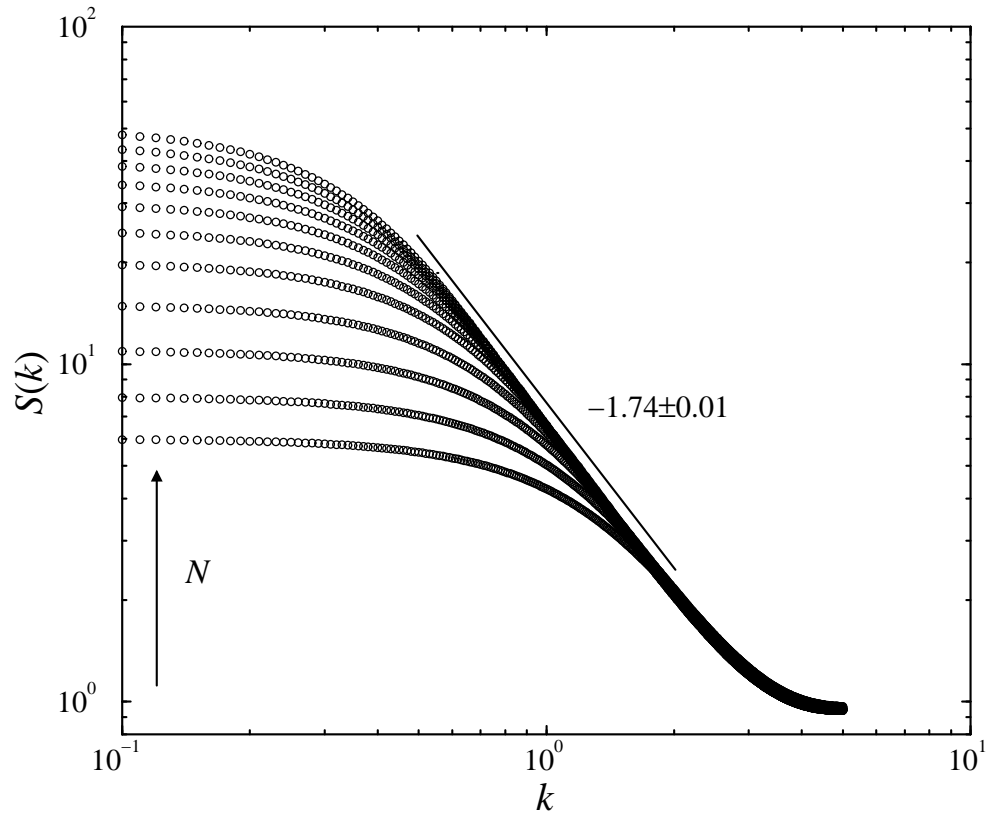


FIG. 8. The static structure factor of the chain, for $N = 6, 8, 11, 15, 20, 25, 30, 35, 40, 45, 50$. The chain length increases along the arrow.

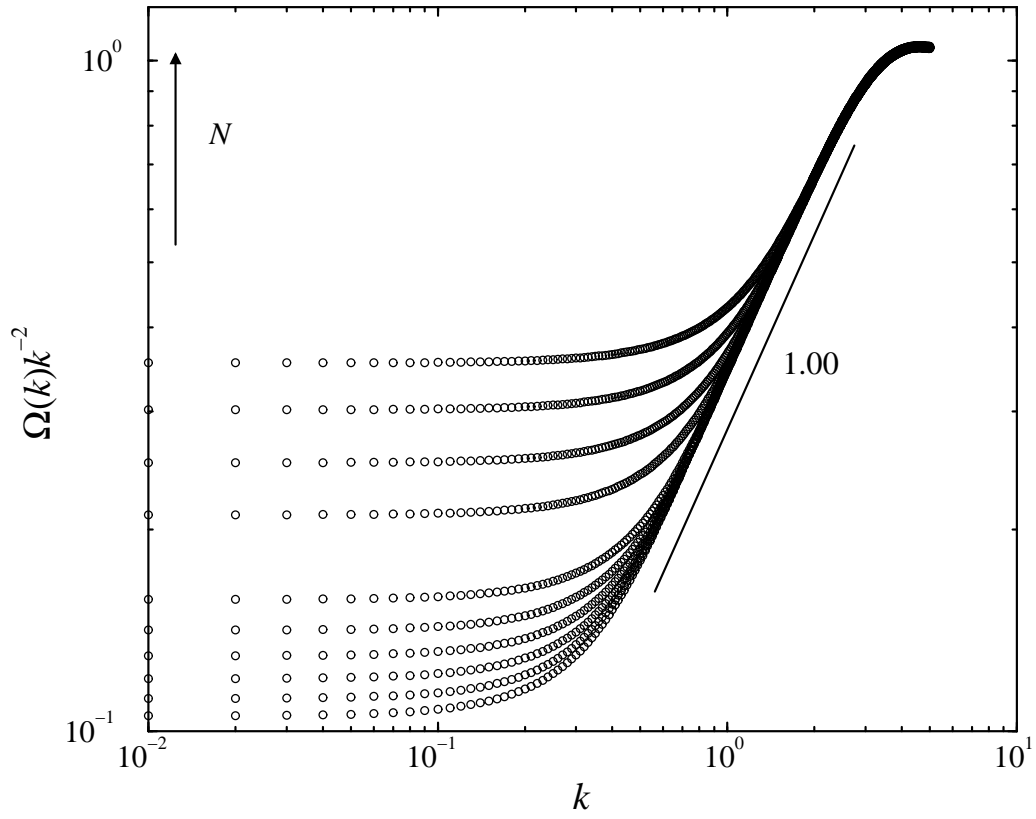


FIG. 9. $\Omega(k)/k^2$ vs. k for $N = 6, 8, 11, 15, 20, 25, 30, 35, 40, 45, 50$. The chain length increases along the arrow.

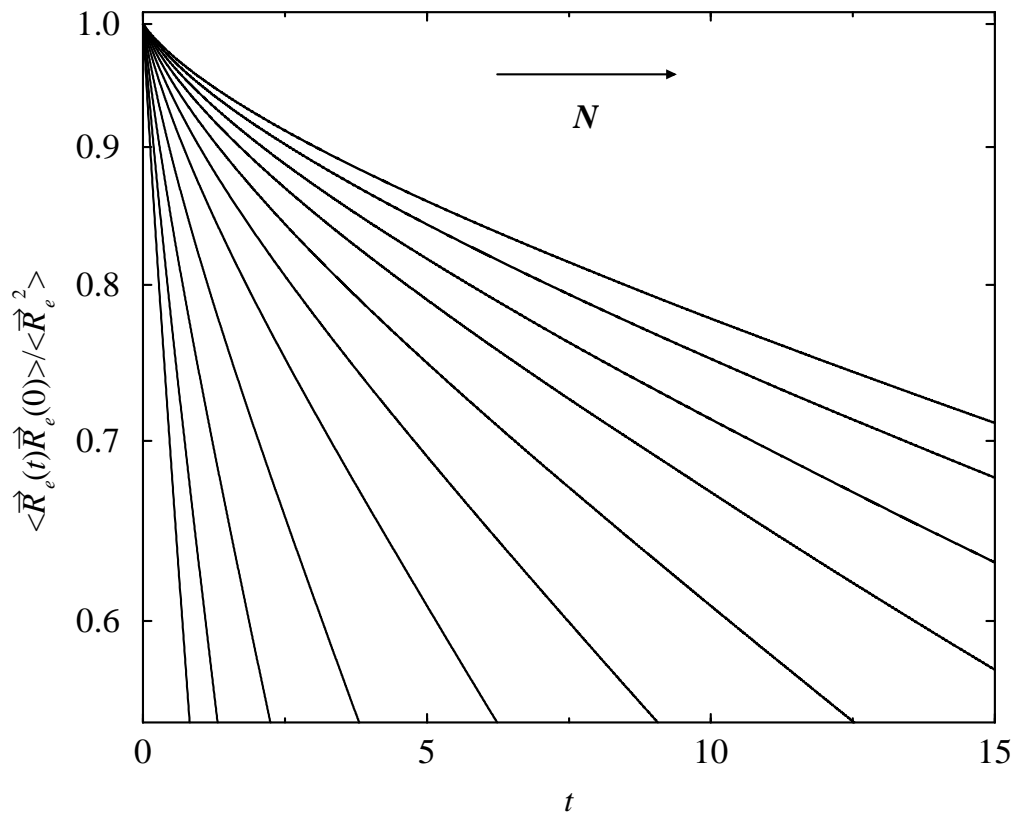


FIG. 10. Normalized autocorrelation function of the end-to-end vector \vec{R}_e for $N = 6, 8, 11, 15, 20, 25, 30, 35, 40, 45, 50$. The chain length increases along the arrow.

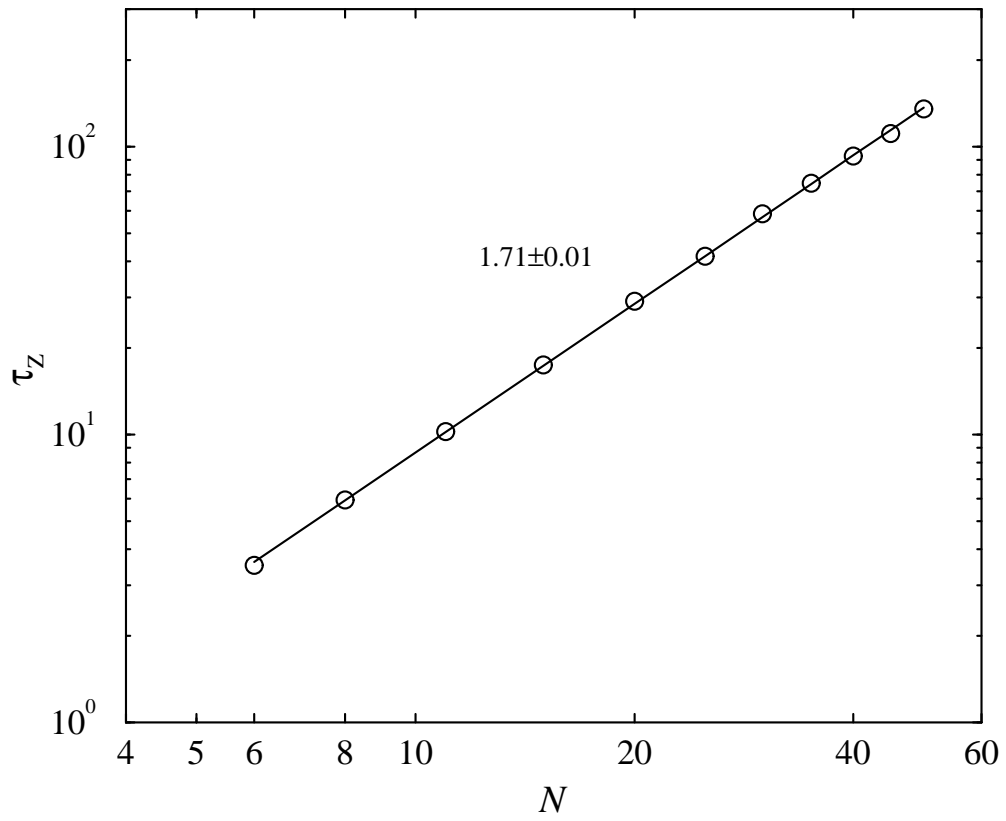


FIG. 11. Chain length scaling for τ_Z obtained from the autocorrelation function of the end-to-end vector. The error bars are smaller than the symbol size.

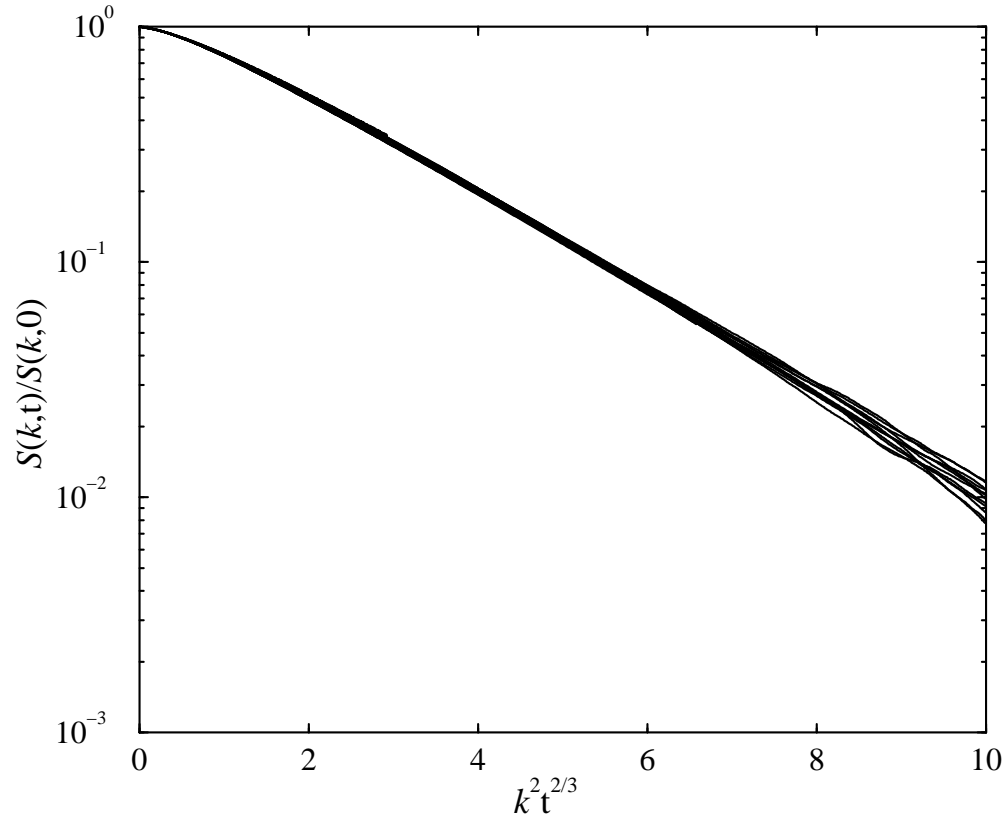


FIG. 12. Log-linear scaling plot of the decay of the dynamic structure factor for $N = 15, 20, 25, 30, 35, 40, 45, 50$ for Zimm scaling: $S(k,t)/S(k,0)$ vs. $k^2 t^{2/3}$. We restricted the wave numbers to the values $k = 1.0, 1.5, 2.0$, and the time regime to $5 \leq t \leq 20$.